Journal of Mines, Metals and Fuels, *71(12): 2414-2425; 2023. DOI: 10.18311/jmmf/2023/34116*

Print ISSN : 0022-2755

Journal of Mines, Metals and Fuels

Contents available at: *www.informaticsjournals.com/index.php/jmmf*

Development of a Multiplication Factor for the Kuz-Ram Model to Match the Fragment Size Obtained from Wipfrag Image Analysis

Rajesh Kumar Das*, Prakash Y. Dhekne and Sunny Murmu

Department of Mining Engineering, National Institute of Technology, Raipur - 492010, Chhattisgarh, India; dasrajesh2001@gmail.com

Abstract

The degree to which the rock is fragmented by blasting operations significantly impacts the productivity of the opencast mining operation. Over image analysis-based tools, the Kuz-Ram empirical model is preferred for determining the mean fragment size of a blasted muck pile. The fragmentation analysis results by the Kuz-Ram model are said to report the overestimation of the size of the fragments. On the other hand, while accurate, measuring the mean fragment size by image-based analysis is also time-consuming and expensive. Therefore, in the present research, the fragmentation difference index (Fdi) is introduced as a new multiplication factor to reduce the discrepancy in the results obtained using the Kuz-Ram model and the image-based analysis. The error minimization method of least squares is used to formulate the objective function of Fdi. The proposed equation is tested using data sets that weren't used in the model's development. Statistical indicators viz. the coefficient of determination (R^2) and Root Mean Square Error (RMSE) have been used to evaluate the model's performance. These are found to be 0.80 and 0.007, respectively. The values obtained by multiplying Fdi by the Kuz-Ram results match those of the Wipfrag study, with an average error of 2.09%. Therefore, the suggested methodology will assist the field engineers in cost-effectively calculating the mean fragment size before blasting utilizing only the findings from the Fdi and Kuz-Ram models..

Keywords: Blasting, Blast Fragmentation, Kuz Ram Model, Mean Fragment Size, Statistical Analysis, WipFrag Image Analysis,

1.0 Introduction

Due to its low cost for quarrying or open cast mining, drill and blast is the most popular method of fragmenting rocks[1-3]. The use of loading, crushing, and transportation machinery is dictated by the overall rock fragment size obtained from blasting. A rock that has been efficiently broken up requires less energy to load or crush. Additionally, it offers properly filling the dumper's payload capacity and well-graded run-of-the-mill to feed the crusher[4].

Numerous researchers have developed methods for predicting the mean fragment size in the muck pile before drilling and blasting operations considering the significance of rock fragmentation which is summarized in Ouchterlony and Sanchidrián 2019[5]. Kuznetsov conducted research in the quantification of rock fragmentation through the development of the Rosin and Rammler distribution function[6]. Later, Cunningham[7] combined the Kuznetsov, Rosin, and Rammler distribution functions to create the Kuz-Ram Model, which is currently widely employed.

The Kuz-Ram Model is often used to estimate the mean fragment size in the blasted muck pile. Its simplicity of use is one of its strongest points. The model can accurately assess the size of the coarse fragments,

**Author for correspondence*

but it may overestimate the size of fines in a muck pile. Additionally, the findings of implementing the Kuz-Ram Model for non-homogenous rocks are determined to be inadequate. Several researchers have noted that the Kuz-Ram Model typically overestimates the size of the fragment[4,8,9].

Numerous computer-aided image analysis approaches have just been developed to determine the distribution of rock fragments in the muck pile. Softwares like Wipfrag, Fragscan, Blastfrag, Split Resultop, etc. are only a few examples[10,11]. The technique for analyzing images has minimal drawbacks, none of which are related to sample quantity or have an adverse effect on production. Furthermore, through the employment of digital cameras or Utility Aerial Vehicles (UAVs), it renders itself for automation. Despite being more accurate than empirical models, the findings from the image-based analytical technique have several inherent drawbacks. The first type of error is one that the image processing program itself is prone to. Second, the technique is only applicable once blasting has taken place and a muck pile has formed. As a result, it does not render fragmentation prediction at the design stage. Therefore, the blast design cannot be created beforehand to get the intended outcome. Thirdly, the program is very expensive and requires a lot of technical knowledge to be utilized. Additionally, it takes time and effort to capture images of the muck pile. Due to all of these factors, field engineers prefer to regulate the blast design based on empirical models for the prediction of rock fragmentation[12].

According to Ouchterlony and Sanchidrián (2019), numerous scholars have noted the discrepancy between the mean fragment size obtained through the implementation of the Kuz-Ram empirical model and the Wipfrag image analysis[5]. By establishing a straightforward equation, this research seeks to reduce the discrepancy between the results of mean fragment size obtained through the implementation of the Kuz-Ram Model and the image-based analytical software, i.e. Wipfrag. The formula takes advantage of Wipfrag's intricacy and precision as well as the Kuz-Ram Model's ease of use. As a result, it can quickly estimate the mean fragment size in a muck pile using a straightforward calculation using the Kuz-Ram Model, all without having to carry out the time-consuming task of image capture or shell out money for pricey tools like Wipfrag. The steps taken to accomplish the aim of the research are described in the section that follows.

2.0 Materials and Methods

In this research, data set from twenty-three production blasts have been compiled to fulfill the aim of the study. The production blasts have been conducted in two opencast limestone mines viz. Rawan Mine is a captive mine belonging to M/S Ambuja Cements Ltd and Rawan Jhipan Mine is captive to M/S UltraTech Cement. The mines are located around 40 km from Raipur, Chhattisgarh. The present topography of the lease area of both mines consists of pits/trenches, dumps, rehabilitation of dumps, roads, plants, buildings, green belts, and plantations. The annual capacity of the Rawan-Jhipan Limestone mine with all clearances in hand is 7.50 million tonnes of limestone and Rawan Limestone mine is 6.31 million

Table 1. Mean geotechnical properties the deposits

Property	Mean (Rawan-Jhipan Limestone Mine)	Mean (Rawan Limestone Mine)
Uniaxial compressive strength, MPa	43.97	42.99
Density, g/cc	2.40	2.38
Porosity, %	5.00	5.00
Young's modulus of elasticity, GPa	50.00	49.14
Spacing between the vertical joints, m	2.00	1.50
Spacing between the horizontal joints, m	1.00	0.90

Table 2. Excavation details

Details	Rawan-Jhipan Limestone Mine	Rawan Limestone Mine
No. of blocks in which Mine is worked	2	2
No benches	4	4
Nature of the first bench	Limestone boulders embedded in clay	Limestone boulders embedded in clay
Height of the first bench, m	0.5-1.5	0.5-1.5
Height of other benches, m	8-11	8-11
Production benches	2nd and 3rd	2nd and 3rd
Orientation of faces	Strike of the vertical joints at 50^{o}-60^{o}	Strike of the vertical joints at 50^{o}-60^{o}
Excavators and their capacity	Hydraulic shovels having a capacity of 6.5 m^3	Hydraulic shovels having a capacity of 6.5 m^3
Dumpers capacity, te	60	60

Table 3. Summary of drill and blast practice

Excavation Details	Rawan-Jhipan Limestone Mine	Rawan Limestone Mine
Drilling machine	Pneumatically operated	Pneumatically operated
Diameter of the holes, mm	152	115 and 152
Burden, m	4.00 to 4.50	3.00 to 3.50 for 115 mm diameter holes and 4.00 to 4.50 for 152 mm diameter holes
Spacing, m	6.50-7.00	5.00 to 5.50 for 115 mm diameter holes and 6.50 to 7.00 for 152 mm diameter holes
Pattern	Staggered	Staggered
Number of rows	2	2
No of holes in a row	15-20	15-20
Explosive used	Site Mixed Emulsion	Site Mixed Emulsion
Initiation method	Shock Tube	Shock Tube
Hole-to-hole delay, ms	25	25
Row to row	42	42
Down-the-hole delay, ms	250	250
The maximum feed size of the crusher, m	1.2	1.2
Secondary rock breakage technique	Hydraulic hammer	Hydraulic hammer.

tonnes of limestone. The mined ore from both mines is fed to the cement plant. The limestone deposit in both mines has a simple topography. The horizontal beds of limestone are mostly overlain by soil, overburden of clay, a gravelly lateritic material, etc. The thickness of the overburden is 0.5 m to 1.5 m. The limestone is fine-grained. There are two major joint sets in each of the mines. The dip of the joints is more than 80°. In addition to these joint sets, bedding joints are also observed in the deposits. The deposits are further crisscrossed by numerous fractures. The joint crevices in the top bench of both mines are filled with weathered breccias whereas they are found open in the lower benches. Water flow is not noticed in the deposits except during the rainy season. The mean geotechnical properties of the deposits, important for fragmentation, are given in Table 1.

The geotechnical properties indicate that the rockmass in both mines is similar. The excavation details of both mines are given in Table 2.

The exploitation of the limestone is done by conventional drilling and blasting methods. The technology for drilling and blasting in both mines is identical. The method adopted in each of the mines is summarised in Table 3.

The firing pattern of the holes is depicted in Figure 1 and Figure 2 shows a typical muck pile.

The blast design associated with the data sets have been shown in Table 4.

Initially, the Kuz-Ram model has been employed to find out the mean fragment size ($X_{50(KR)}$) using the data set from Table 1 before the blasting events. After that, the Wipfrag software was employed for image analysis of

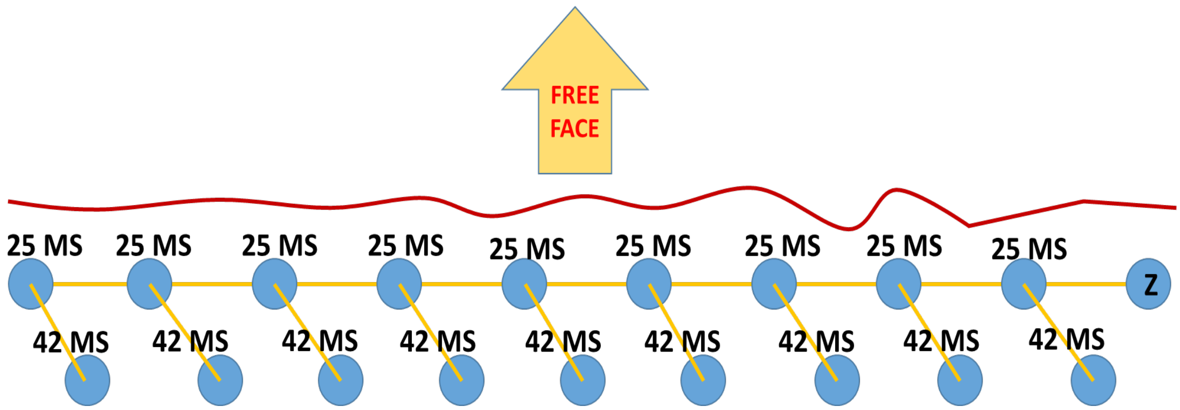

Figure 1. Typical firing pattern adopted for a bench blast.

Figure 2. Muck profile achieved after blasting.

Table 4. The blast design implemented for the current study

Sl. No.	Hole dia. (mm)	No. of holes	Burden (m)	Spacing (m)	Depth of hole (m)	Powder factor (m^3/kg)	Charge per hole (kg)	$X_{50(KR)}$ (m)	$X_{50(Wf)}$ (m)
1.	152	45	4.00	6.50	7.00	6.13	74.20	46.04	21.597
2.	152	54	4.00	6.50	8.00	6.10	85.19	46.94	21.623
3.	152	28	4.00	6.50	7.30	6.62	71.64	48.68	33.012
4.	152	20	3.80	6.50	7.30	6.01	75.00	45.39	18.628
5.	152	40	4.00	7.00	8.20	6.28	91.45	48.56	30.168
6.	152	24	4.00	7.00	8.30	6.18	94.00	48.19	27.805
7.	152	22	4.00	7.00	8.50	6.25	95.23	48.71	33.434
8.	152	30	4.00	6.50	7.00	6.33	71.90	46.97	22.353
9.	152	40	4.00	6.50	7.00	6.42	70.88	47.40	26.247
10.	152	19	3.75	6.50	7.40	6.42	70.26	47.32	23.164
11.	115	35	3.00	5.40	8.20	5.17	64.20	39.23	33.556
12.	115	48	3.00	5.50	7.50	5.19	59.56	38.87	33.02
13.	115	48	3.00	5.00	7.50	5.06	55.63	37.61	29.793
14.	115	46	3.00	5.50	7.80	5.90	54.57	42.40	42.391
15.	115	28	3.00	5.50	8.50	5.26	66.68	40.00	35.322
16.	115	19	3.50	5.50	8.00	5.63	68.42	42.41	42.303
17.	115	20	3.00	5.00	7.50	5.02	56.00	37.45	28.108
18.	115	15	3.00	5.50	8.10	5.71	58.53	41.80	35.426
19.	115	15	3.40	5.50	8.00	5.55	67.33	41.86	38.465
20.	115	17	3.00	5.40	8.00	5.25	61.76	39.42	34.900
21.	115	33	3.50	4.00	7.70	5.00	54.00	31.59	30.790
22.	115	38	3.50	4.00	7.00	5.40	49.00	32.86	35.440
23.	115	42	3.50	4.00	7.00	5.40	49.00	32.86	35.230

the blasted muck pile. The resultant mean fragment size obtained from Wipfrag analysis is termed $X_{50(Wf)}$.

2.1 Kuz-Ram Model

As was already indicated, the Kuz-Ram empirical model continues to be widely used to predict the mean fragment size before a blasting event. Nevertheless, there are many shortcomings associated with it. The field engineers, however, rather favor it because of its simplicity. It is desired that the model be enhanced to match the outcomes of image analysis. The Kuz-Ram model takes into account four crucial elements when evaluating blast fragmentation: blast geometry, explosive properties, explosive quantity, and rock factor. By taking into account a muck pile's 50% passage of the amount of blasted material, the Kuz-Ram model calculates the mean fragment size.

Kuznetsov first suggested the Kuz-Ram model, which Cunningham[13] later adjusted to predict the likely mean fragment size ($X_{50(KR)}$) of the resultant muck pile obtained after blasting. The empirical model includes three main equations: (i) the Kuznetsov equation, (ii) Rosin-Rammler's equation, and, (iii) the uniformity index as shown in Equation (1)-(3).

$$X_{50(KR)} = A \times K^{-0.8} \times Q^{1/6} \times \left[\frac{115}{RWS}\right]^{\frac{19}{30}} \tag{1}$$

Where, $X_{50(KR)}$ is the mean fragment size of the muck pile (cm), A is the rock factor, K is the powder factor in (kg/m^3), Q is the explosive weight in the blast hole (kg), and, RWS is the weight strength of the explosive related to Ammonium Nitrate (ANFO). The Rosin-Rammler distribution was used to assess the proportion of muck pile passing through a given opening size of a screen as given in Equation (2).

$$R(X) = 1 - e^{-\left(\frac{X}{X_c}\right)^n} \tag{2}$$

Where, $R(X)$ is the % passing through a screen opening of size X, the screen size is denoted by X (cm), X_c is the characteristic size (cm), and, n is the uniformity index. Using Equation (3) the uniformity index n can be further calculated as follows as proposed by Cunningham:

Table 5. Parameters used for rock factor calculation and their respective ratings[16]

Notations	Definitions	Ratings
RMD	Rock mass description	
	Powdery/friable	10
	Vertically jointed	20
	Massive	50
JF	Joint factor (JPS+JPA)	
JPS	Vertical joint spacing	
	<0.1m	10
	0.1m to oversize	20
	Oversize to drilling pattern size	50
JPA	Joint plane angle	
	Dip out of the face	20
	Strike perpendicular to the face	30
	Dip into face	40
RDI	Density influence	25 x ρ_T-50
HF	Hardness factor	
	If Young's modulus (E) < 50 GPa	HF = 0.3333E
	If E > 50 MPa	HF = 0.25 x unconfined compressive strength

$$n = \left[2.2 - \frac{14B}{d}\right]\left[\frac{1}{2} + \frac{S}{2B}\right]^{0.5}\left[1 - \frac{w}{B}\right]\left[\frac{L}{H}\right]P \quad (3)$$

Where, n is the uniformity index, B is the burden (cm), d is the hole diameter (mm), S is the spacing (m), w is the standard deviation of drilling precision (m), L is the charge length (m), H is the bench height (m), and, P is the factor of staggered drilling pattern.

'*n*' (Equation (3)) depends upon the blast design parameters. Its value generally ranges from 0.8 to 1.5. As the value of the '*n*' increases the fragmentation distribution in a muck pile becomes more non-uniform.

The characteristic size (X_c) of the fragments obtained using the Rosin-Rammler Distribution (Equation (2)) is obtained using Equation (4).

$$X_c = \frac{X_{50}}{(0.693)^{\frac{1}{n}}} \quad (4)$$

Cunningham[7] adjusted the rock factor by linking it to the blastability index proposed by Lilly[14] as presented in Equation (5). It was suggested by him that the rock factor depends upon the geo-technical parameters of the rock[14,15]. The explanation and the assigned ratings of various parameters in Equation (5) are presented in Table 3. The rock factor , can further be calculated using Equation (5) as described below:

$$A = 0.06(RMD + JF + RDI + HF) \quad (5)$$

Where, *RMD* is the rock mass description, *JF* is the joint factor, *RDI* is the rock density influence, and, *HF* is the hardness factor. Furthermore, the different parameters for determining rock factor are shown in Table 5. Moreover, the sieving result of fragment size distribution is shown in Figure 3.

2.2 Image Analysis: Wipfrag

The Wipfrag software was selected to carry out image analysis. The basic procedures for image analysis are: (a) digital videography (b) image capture (c) picture opening in Wipfrag software (d) scale setting (e) generation of nets (f) edge detection (g) sieving. Following the instructions in the Wipfrag user manual, Maerz, *et al.*, and Wimmer and Ouchterlony, the images were captured with a digital camera[17,18]. Several images of a single muck pile were taken in order to accurately capture its spread and depict the distribution of the blasted muck pile. Wipfrag can be used to generate the size, perimeter, shape, and orientation of the muck pile's geometry in two dimensions. The Wipfrag software's edge detection provides a polygon network around each particle so that fragmentation results can be achieved instantaneously. Some of the digital results of image analysis using Wipfrag software are shown in Figures 3(a)-(c).

2.3 Development of the Multiplication Factor

A new index namely Fragmentation difference index (Fdi) is introduced, which is the ratio between the results obtained from Wipfrag and the Kuz-Ram model and can be written as:

$$Fdi = \frac{X_{50(Wf)}}{X_{50(KR)}} \quad (6)$$

The value Fdi range between 0 to 1. If Fdi is close to 1, it suggests that the mean fragment size results obtained from the Kuz-Ram model are equal to the mean fragment size obtained from the Wipfrag analysis. However, if Fdi is close to 0 then, it denotes that the difference between the mean fragment size result obtained from the Kuz-Ram model and Wipfrag is quite significant. Therefore, Fdi acts as a multiplication factor to the Kuz-Ram model to equate the results to the Wipfrag analysis.

Initially, simple regression plots were applied using 18 data sets out of 23 data sets to find out the relationship between *Fdi* and blast design parameters and explosive parameters whereas the remaining 5 data sets were reserved for validation. It was observed that *Fdi* had a good linear correlation with the average depth of the blast hole (*D*), the charge per hole (C_{hole}), and, Spacing to burden ratio (S/B). Therefore, the following equation was proposed (Equation (7)):

$$Fdi = \alpha.D + \beta.C_{hole} + \gamma.\frac{S}{B} \quad (7)$$

Where, α, β, and, γ are the constants. Then, the least square method of error minimization was adopted to determine the values of the constants aforementioned as follows (Equation (8)):

$$E(\alpha,\beta,\gamma) = \sum\left[Fdi_{obs} - \left(\alpha.D + \beta.C_{hole} + \gamma.\frac{S}{B}\right)\right]^2 \quad (8)$$

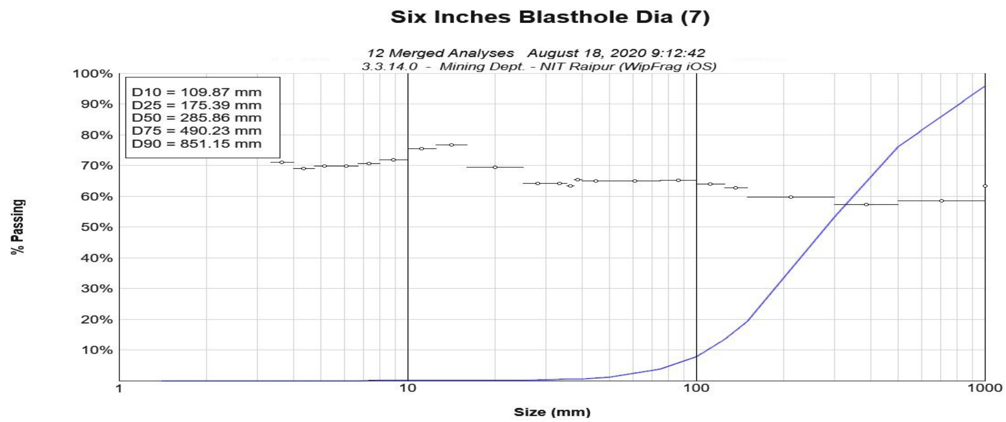

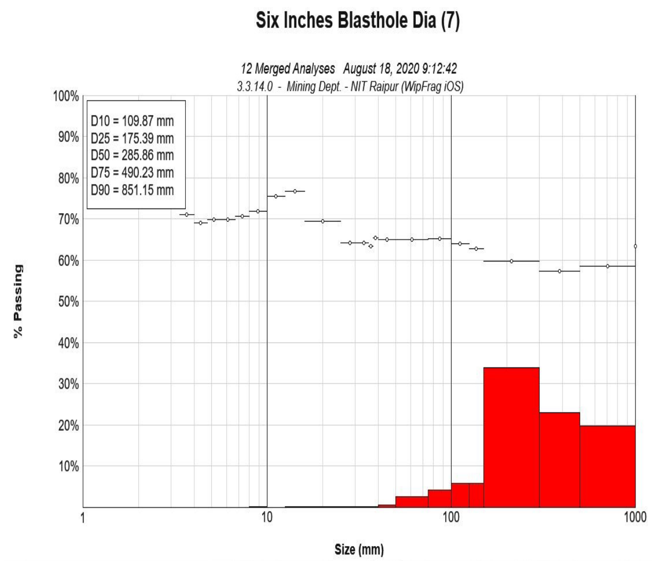

Size (mm)	% Passing
1000.00	95.88%
500.00	76.12%
300.00	53.20%
150.00	19.25%
125.00	13.44%
100.00	7.76%
75.00	3.68%
50.00	1.12%
40.00	0.61%
37.50	0.50%
35.50	0.44%
31.50	0.33%
25.00	0.19%
16.00	0.09%
12.50	0.06%
10.00	0.04%
8.00	0.02%
6.70	0.01%
5.60	0.00%
4.75	0.00%
4.00	0.00%
3.35	0.00%
2.00	0.00%
1.40	0.00%
1.00	0.00%

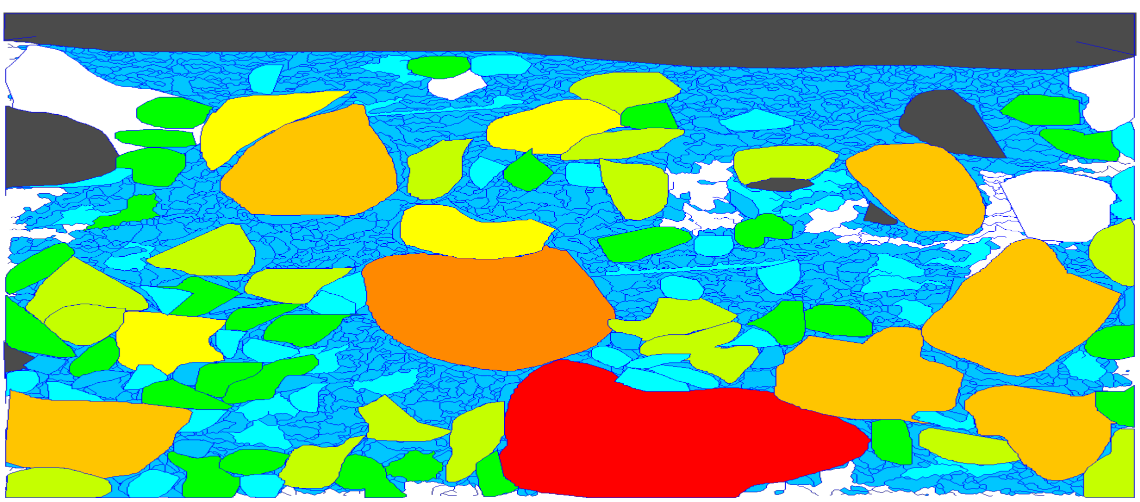

Figure 3. Figures showing: **(a)** Cumulative probability distribution of fragment size. **(b)** probability density of fragment size. **(c)** Digital image of a muck pile.

Where, E is the error function and it can be minimized if it satisfies the following partial differentiation (Equation (9)):

$$\frac{\partial E}{\partial \alpha} = 0; \frac{\partial E}{\partial \beta} = 0; \frac{\partial E}{\partial \gamma} = 0 \tag{9}$$

After solving the partial differentiation, the regression model for Fdi was obtained as:

$$Fdi = 0.296.D - 0.013.C_{hole} - 0.339.\frac{S}{B} \tag{10}$$

Thus, Equation (6) can be rewritten as:

$$X_{50(Wf)} = \left[0.296.D - 0.013.C_{hole} - 0.339.\frac{S}{B}\right] \times X_{50(KR)} \tag{11}$$

Therefore, before any blasting event if the values of D, C_{hole}, S/B, and, $X_{50(KR)}$ are known then, one can easily determine the value $X_{50(Wf)}$ without even having to purchase the costly Wipfrag software and conducting the tedious task of digital videography and image capturing and garnering expertise to use the sophisticated software. Hence, the accuracy of fragmentation of a blasted muck pile can be easily calculated using a simple formula shown in Equation (11).

The statistical significance of the proposed regression model of Fdi can be established by assessing the values of coefficient of determination (R^2), Root Mean Square Error (RMSE), and, *p*-value concerning the partial F-Test. The Analysis of Variance (ANOVA) of the regression analysis is summarized in Table 3. The R^2 of the model has been determined based on the sum of squared residual and the total sum of squared values, as given below in Equation (12).

$$R^2 = 1 - \frac{RSS}{TSS} \tag{12}$$

Where, *RSS* and *TSS* are the residual sum of squared error and the total sum of squared error along with the summary of regression are mentioned in Tables 4 and 5. The Root Means Square Error (RMSE) can be computed using the following equation (Equation 13):

$$RMSE = \sum_{1}^{N} \frac{\left[Fdi_{pred} - Fdi_{obs}\right]^2}{N} \tag{13}$$

Where Fdi_{pred},, Fdi_{obs}, and N are the predicted, observed values of Fdi and total no. of observations respectively. Also, MSR (Mean Sum of squared Regression) and MSE (Mean Sum of squared Error) have been used to compute the '*F*' statistic of the model, as given in equation (Equation 14).

$$F\ statistics = \frac{MSR}{MSE} \tag{14}$$

The values of R^2 and RMSE were determined to be 0.80 and 0.007 respectively. The computed *F* statistics were also found to be less than the critical value of *F* statistics obtained from the *F* distribution table as per the significance level of 95%. The *p*-value in the ANOVA was also found to be less than 0.05. An empirical model possessing an R^2 value of greater than 0.70 and RMSE close to 0 is regarded to have a strong prediction capability[19,20]. Given the aforementioned criteria, the regression model of stands statistically significant. Table 6 presents the summary of regression statistics and Table 7 presents analysis of variance.

Table 6. Summary of regression analysis

Regression Statistics	
Multiple R	0.895939
R Square	0.802707
Adjusted R Square	0.76043
Standard Error	0.096279
Observations	18

Table 7. Analysis of variance

	Degree of freedom	Sum of square	Mean sum of square	F statistics	Significance F (*p*-value)
Regression	3	0.528	0.18	18.99	<0.05
Residual	14	0.129	0.009		
Total	17	0.658			

Table 8. Data set for validation purpose

Sl. No.	D (m)	C_{hole} (kg)	S/B				% E
1.	8.5	95.23	1.75	48.71	33.43	33.54	0.32
2.	8	67.33	2.33	41.86	38.46	36.49	5.41
3.	7.7	53.94	1.14	31.59	30.79	30.49	0.96
4.	7	54.16	1.14	32.86	35.44	34.21	3.57
5.	7	44.33	1.14	32.86	35.23	35.16	0.19

As mentioned earlier that five data sets as shown in Table 4 were reserved to validate the proposed Equation (11). It was observed that the error percentage E% as shown in Equation (15) were found to be well within the acceptable limit of <10% respectively[21]. Thus, the proposed model as depicted in Equation (11) stands validated. Table 8 presents the percentage error in predictions by the Wipfrag and the Kuz-Ram model using the *Fdi*

$$E\ \% = \left| \frac{(X_{50(Wf)} - X_{50(Wf,pred)})}{MSE} \right| \times 100 \qquad (15)$$

3.0 Results and Discussions

As mentioned earlier that 18 data sets were utilized to develop the regression model for Fdi. A comparison was made between the data set Kuz-RamModel ($X_{50(KR)}$), Wipfrag analysis ($X_{50(Wf)}$), and, modified mean fragment size as obtained from Equation (10) ($X_{50(Wf,pred)}$). The maximum E% between ($X_{50(KR)}$) and ($X_{50(Wf,pred)}$), was found to be 22.1%. However, the average E% was found to be 2.09, which is minimal and well within the permissible limit. However, the maximum E% between ($X_{50(KR)}$) and ($X_{50(Wf,pred)}$) was found to be 143.67%. In addition, the average E% between ($X_{(50(KR)}$) and ($X_{(50(Wf,pred)}$) was found to be 54.96%, this suggests that the difference between the results obtained using the Kuz-Ram empirical Model is significantly higher. It implies that the Kuz-Ram model predicts the mean fragment size 1.5 times greater than what is computed by WIPFRAG image analysis on average. The difference in the results of each methodology is depicted in Figure 4.

Therefore, the use of the proposed model Equation (11) can significantly reduce the difference between the mean fragment size obtained from Kuz-Ram empirical Model and Wipfrag image analysis by simply introducing a multiplication factor i.e., Fdi. Numerous advantages can be brought by using Equation (10):

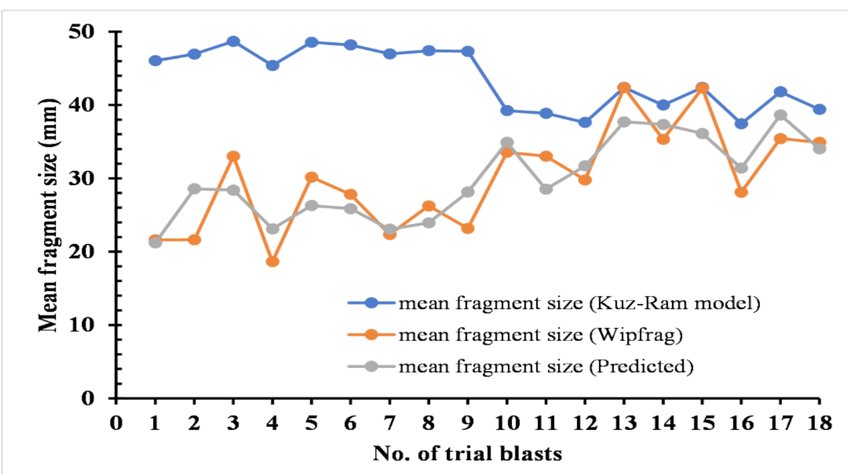

Figure 4. Data set of mean fragment size of the Kuz-Ram model, Wipfrag analysis, and the predicted values.

1. The fragmentation of the muck pile can be predicted in the accuracy of Wipfragimage analysis by calculating the mean fragment size () using Kuz-Ram empirical Model and multiplying the *Fdi* well in advance of blasting.
2. It is simple and user-friendly for field engineers.
3. A lot of time and energy can be saved as the tedious work of capturing videography and multiple images of the blasted muck pile are not required.
4. Significant cost reduction can be achieved as the requirement for a digital camera, Wipfrag software and accessories can be avoided.

4.0 Conclusion

In this study, the disparity between the mean fragment size of the blasted muck pile obtained from the Kuz-Ram empirical Model and Wipfrag image analysis was significantly reduced by introducing a new index known as Fragmentation difference index *(Fdi)*. The prediction of *Fdi* was formulated by employing the least square method of error minimization. It was found that *Fdi* was highly correlated to the average depth of the blasted hole (D), the charge per hole (C_{hole}), and the Spacing-to-Burden ratio (S/B). The statistical significance of the proposed model of *Fdi* was achieved by obtaining R^2 and RMSE of 0.80 and 0.007 respectively. In the validation process, the proposed Model seemed to predict the mean fragment size well within the permissible limit of error. The maximum and the mean percentage error between the Kuz-Ram empirical model value ($X_{50(KR)}$) and Wipfrag image analysis value ($X_{50(Wf)}$) was found to be 143.67% and 54.96% respectively. Furthermore, the maximum and the average percentage error between ($X_{50(KR)}$) and ($X_{50(Wf,pred)}$), were found to be 22.1% and 1.74 % respectively. This implies that the proposed model has helped to significantly reduce the difference between the mean fragment size obtained from Kuz-Ram empirical model and Wipfrag image analysis. Thus, the mean fragment size of a blasted muck pile can be accurately predicted before the blasting event using the proposed model.

5.0 Acknowledegements

The authors wish to acknowledge the management and the persons involved in Drilling and Blasting activities and specially the Blaster and Driller of the Rawan limestone mine of M/s Ambuja Cements and Rawan Jhipan Limestone Mine of M/S Ultratech Cement Limited; Distt: Baloda Bazar for Conducting, granting permission and involved to carry out the investigations.

6.0 References

1. Agrawal A, Choudhary BS, Murthy VMSR, Murmu S. Impact of bedding planes, delay interval and firing orientation on blast induced ground vibration in production blasting with controlling strategies. Meas J Int Meas Confed. 2022; 202:111887. https://doi.org/10.1016/j.measurement.2022.111887
2. Murmu S, Maheshwari P, Verma HK. Empirical and probabilistic analysis of blast-induced ground vibrations. Int J Rock Mech Min Sci. 2018; 103:267–74. https://doi.org/10.1016/j.ijrmms.2018.01.038
3. Maheshwari P, Murmu S, Verma HK. Modeling of blast induced damage distance for underground tunnels. Indian Geotech Conf. 2019; 617–26. https://doi.org/10.1007/978-981-33-6466-0_57
4. Lawal AI. A new modification to the Kuz-Ram model using the fragment size predicted by image analysis. Int J Rock Mech Min Sci. 2021; 138:104595. https://doi.org/10.1016/j.ijrmms.2020.104595
5. Ouchterlony F, Sanchidrián JA. A review of development of better prediction equations for blast fragmentation. J Rock Mech Geotech Eng. 2019; 11:1094–109. https://doi.org/10.1016/j.jrmge.2019.03.001
6. Kuznetsov VM. The mean diameter of the fragments formed by blasting rock. Sov Min Sci. 1973; 9:144–8. https://doi.org/10.1007/BF02506177
7. Cunningham CVB. Fragmentation estimations and the kuz-ram model-four years on. Proc 2nd Int Symp Rock Fragm by Blasting. 1987; 475–87.
8. Hoser AA, Madsen AO. The Kuz-Ram fragmentation model – 20 yearson. Bright Conf Proc. 2005; 201–10. https://doi.org/10.1107/S2053273316018994
9. Spathis AT. A correction relating to the analysis of the original Kuz-Ram model. Fragblast. 2004; 8:201–5. https://doi.org/10.1080/13855140500041697
10. Kabwe E. Velocity of detonation measurement and fragmentation analysis to evaluate blasting efficacy. J Rock Mech Geotech Eng. 2018; 10:523–33. https://doi.org/10.1016/j.jrmge.2017.12.003
11. Ozkahraman HT. Fragmentation assessment and design of blast pattern at Goltas Limestone Quarry Turkey.

Int J Rock Mech Min Sci. 2006; 43:628–33. https://doi.org/10.1016/j.ijrmms.2005.09.004

12. Shehu SA, Yusuf KO, Hashim MHM. Comparative study of WipFrag image analysis and Kuz-Ram empirical model in granite aggregate quarry and their application for blast fragmentation rating. Geomech Geoengin. 2022; 17:197–205. https://doi.org/10.1080/17486025.2020.1720830
13. Cunningham CVB. The Kuz-Ram model for prediction of fragmentation from blasting. Proc 1st Int Symp Rock Fragm by Blasting. Sweden. 1987; 439–57.
14. Lilly PA. An empirical method of assessing rock mass blastability. Proc Large Open Pit Mine Conf Newman. 1986; 89–92.
15. Tosun A, Ongen T, Karakus D, Onur AH. Development of the Kuz-Ram model to blasting in a limestone quarry. Arch Min Sci. 2014; 59:477–88. https://doi.org/10.2478/amsc-2014-0034
16. Adebola JM, Ajayi OD, Peter Elijaho O. Rock fragmentation prediction using Kuz-Ram Model. 2016; 16(5).
17. Wimmer M, Ouchterlony F. 2D image analysis using WipFrag software compared with actual sieving data of Kiruna magnetite loaded from a drawpoint. 2009.
18. Maerz NH. Reconstructing 3-D block size distribu- tions from 2-D measurements on sections. in: FRAGBLAST 5 Work Meas Blast Fragm, Montreal, Canada. 1996; 39–43. https://doi.org/10.1201/9780203747919-7
19. Murmu S, Budi G. A probability-based risk assessment of roof strata weighting in longwall panels. Arbian J Geosci. 2021; 14:362. https://doi.org/10.1007/s12517-021-06637-y
20. Murmu S, Budi G. Study on the mechanism, prediction, and control of coal wall spalling in deep longwall panels utilizing advanced numerical simulation methodology. Geofluids. 2022; 1–19. https://doi.org/10.1155/2022/5622228
21. Dhekne PY, Pradhan M, Jade RK, Mishra R. Boulder prediction in rock blasting using artificial neural network. ARPN Journal of Engineering and Applied Sciences (JEAS). 2017; 12.